

January 10, 2022

off-shell  $t\bar{t}b\bar{b}$  in the di-lepton channelMANFRED KRAUS<sup>1</sup>

*Physics Department, Florida State University  
Tallahassee, FL 32306-4350, U.S.A*

We report on our recent calculation for the off-shell  $t\bar{t}b\bar{b}$  process in the di-lepton decay channel at the LHC. Our results take into account NLO QCD corrections for the complete  $pp \rightarrow e^+ \nu_e \mu^- \bar{\nu}_\mu b\bar{b}b\bar{b}$  process, and include all double, single and non-resonant contributions. We investigate the size of the corrections and their associated theoretical uncertainties. We also briefly comment on the impact of different  $b$  jet definitions on our results.

PRESENTED AT

14<sup>th</sup> International Workshop on Top Quark Physics  
(videoconference), 13–17 September, 2021

---

<sup>1</sup>Work is supported in part by U.S. Department of Energy under grant DE-SC010102

# 1 Introduction

With the discovery of the Higgs boson at the LHC the focus of the physics programs lies on the precise investigation of fundamental properties of the Higgs boson and its interactions. In that context the top-quark Yukawa coupling is of special interest as the top-quark is the heaviest fundamental particle in the Standard Model. To probe directly the top-higgs interactions it is beneficial to study the Higgs boson production in association with a top-quark pair. In order to compensate for the small production rate of the  $pp \rightarrow t\bar{t}H$  process the decay of the Higgs boson into bottom quarks,  $H \rightarrow b\bar{b}$ , is of special interest as it has the largest branching ratio.

To measure precisely the  $pp \rightarrow t\bar{t}H(H \rightarrow b\bar{b})$  signal multiple challenges have to be overcome. For instance, once also the top-quarks decay the final state consists out of four  $b$  jets, which generates the combinatorical problem of the  $b$  jet assignment in the reconstruction of the Higgs boson. On the other hand, large Standard Model background processes have to be under excellent theoretical control to isolate signal events. The main background contributions consists out of the QCD production of the  $pp \rightarrow t\bar{t}b\bar{b}$  process at  $\mathcal{O}(\alpha_s^4)$ . Similarly, due to the presence of the four  $b$  jets in the decayed signature,  $pp \rightarrow t\bar{t}b\bar{b}$  also affects searches for the four top-quark production at the LHC. Thus, measurements of  $pp \rightarrow t\bar{t}H(H \rightarrow b\bar{b})$  and  $t\bar{t}t\bar{t}$  will benefit from a better understanding of the QCD production of the  $pp \rightarrow t\bar{t}b\bar{b}$  process as well as the improved description of top-quark decays.

The  $t\bar{t}b\bar{b}$  process has been extensively studied in the literature at NLO QCD accuracy. For instance, for on-shell  $t\bar{t}b\bar{b}$  the next-to-leading order QCD corrections are available [1–5] for over 10 years by now. The impact of parton shower matching has been also thoroughly addressed in Refs. [6–10]. Furthermore,  $t\bar{t}b\bar{b}/t\bar{t}jj$  cross section ratios have been investigated in Ref. [11] as well as the  $t\bar{t}b\bar{b}$  production in association with a hard jet [12] has been computed at NLO QCD accuracy. In all the aforementioned studies top-quarks have been treated as stable particles and top-quark decays have been included at most at LO accuracy. Only recently the computation of NLO QCD corrections for the full off-shell process in the di-lepton channel [13, 14] has become feasible. These calculations include for the very first time also NLO QCD corrections to the top-quark decays and double, single and non-resonant contribution as well as interference effects. Here we report on our recent calculation for the full off-shell production of the  $pp \rightarrow t\bar{t}b\bar{b}$  process [13] including leptonic top-quark decays.

## 2 Outline of the calculation

In the following we will briefly summarize the outline of the calculation. For more details we refer the reader to the original publication [13]. We compute NLO QCD corrections for the  $pp \rightarrow e^+ \nu_e \mu^- \bar{\nu}_\mu b\bar{b}b\bar{b}$  process at  $\mathcal{O}(\alpha^4 \alpha_s^5)$  for the LHC operating at a

center-of-mass energy of  $\sqrt{s} = 13$  TeV. The computation is based on matrix elements for the fully decayed final state that comprise not only the double resonant  $t\bar{t}b\bar{b}$  production, but also single and non-resonant contributions, for which representative diagrams are shown in Fig. 1. In addition, the matrix elements also account for

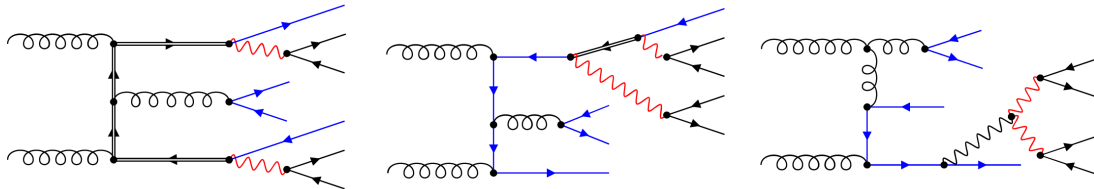


Figure 1: Representative Feynman diagrams for double, single and non-resonant contributions in the  $pp \rightarrow b\bar{b}b\bar{b}e^+\nu_e\mu^-\bar{\nu}_\mu$  matrix elements. Figure taken from Ref. [13]

finite width effects of unstable particles and interference effects between the various contributions. The calculation is performed using the HELAC-NLO framework [15] that has been already employed in various full off-shell computations at NLO QCD accuracy for  $t\bar{t}V$  processes [16–20]. The framework consists out of HELAC-1LOOP [21–23] for the computation of virtual one-loop corrections and HELAC-DIPOLES [24–26] that takes care of the infrared subtraction for radiative corrections.

We investigate a fiducial signature consisting out of at least four  $b$  jets, two charged leptons and missing energy. Jets are formed using the anti- $k_T$  jet algorithm [27] with a separation parameter of  $R = 0.4$ . We employ the following inclusive phase space cuts

$$p_T(\ell) > 20 \text{ GeV} , \quad p_T(b) > 25 \text{ GeV} , \quad |y(\ell)| < 2.5 , \quad |y(b)| < 2.5 . \quad (1)$$

### 3 Phenomenological results

Let us start our discussion with the inclusive cross section. In Tab. 1 LO and NLO integrated cross sections are shown for two different choices of renormalization and factorization scales  $\mu_R = \mu_F = \mu_0$ , namely a fixed scale  $\mu_0 = m_t$  and a dynamical one  $\mu_0 = H_T/3$ . Also shown are scale uncertainties estimated from independent variations of the renormalization and factorization scales as well as PDF uncertainties. We find that the NLO QCD corrections are large and of the order +90%. At the same time the residual scale dependence reduces roughly by a factor of 3 from 60% at LO down to the level of 20% at NLO. Given the still sizable scale uncertainties at NLO the PDF uncertainties, which are of the order of  $\pm 1\%$  are negligible. Our findings are the same independent of the nature of the employed renormalization and factorization scale. However, for differential distributions we only show results for the dynamical

$\mu_0$	$\sigma^{\text{LO}}$ [fb]	$\delta_{\text{scale}}$	$\sigma^{\text{NLO}}$ [fb]	$\delta_{\text{scale}}$	$\delta_{\text{PDF}}$	$\mathcal{K} = \sigma^{\text{NLO}}/\sigma^{\text{LO}}$
$m_t$	6.998	+4.525 (65%) -2.569 (37%)	13.24	+2.33 (18%) -2.89 (22%)	+0.19 (1%) -0.19 (1%)	1.89
$H_T/3$	6.813	+4.338 (64%) -2.481 (36%)	13.22	+2.66 (20%) -2.95 (22%)	+0.19 (1%) -0.19 (1%)	1.94

Table 1: LO and NLO integrated fiducial cross sections for the  $pp \rightarrow e^+ \nu_e \mu^- \bar{\nu}_\mu b\bar{b} b\bar{b}$  process at the LHC with  $\sqrt{s} = 13$  TeV.

scale  $\mu_0 = H_T/3$ , as it is well known that a fixed scale can not capture the behaviour of the high-energy tails appropriately.

Next we discuss the impact of NLO QCD corrections at the differential level. In Fig. 2 we show the differential cross section distribution of the transverse momentum of the hardest  $b$  jet and of the muon. Even though the transverse momentum of the

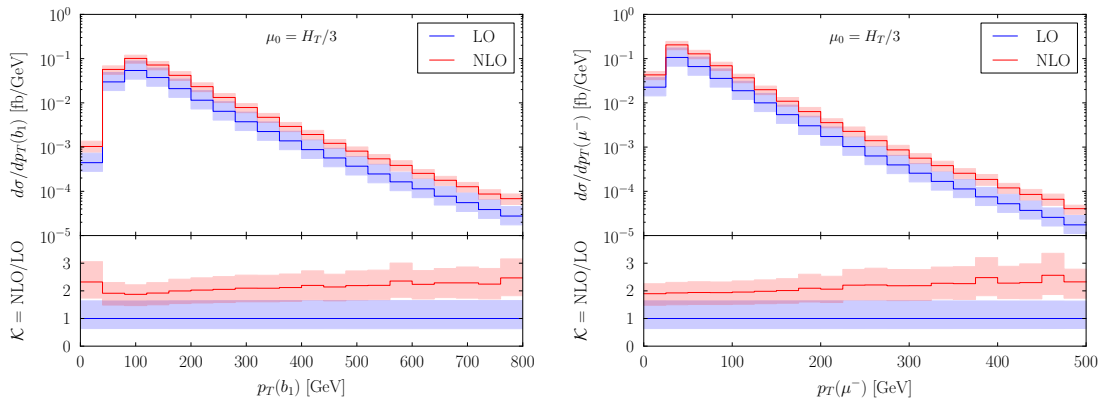


Figure 2: Differential cross section distribution for the transverse momentum of the hardest  $b$  jet (l.h.s) and of the muon (r.h.s). Plots taken from Ref. [13].

hardest  $b$  jet is a hadronic observable, whereas the transverse momentum of the muon is a purely leptonic one they are affected very similar from NLO QCD corrections. The corrections are large over the whole plotted range and increase in the tail of the distribution. Thus the NLO K-factor is far from being flat. Furthermore, we notice that the scale uncertainty bands are barely overlapping and have similar sizes suggesting a strong impact from real radiation processes that are only taken into account at LO accuracy.

We have also investigated PDF uncertainties at the differential level, which are at the level of a few percent for most observables. However, in extreme cases they can

be as large as  $\pm 10\%$ . We refer the reader to our publication [13] for more details.

At last, we also estimated the impact of different definitions of  $b$  jets on our results. We consider the two cases where one can either distinguish between  $b$  and  $\bar{b}$  or not. This leads to the following recombination rules for the jet algorithm

$$\begin{aligned} \text{charge-blind:} & \quad bg \rightarrow b, \bar{b}g \rightarrow \bar{b}, b\bar{b} \rightarrow g, bb \rightarrow g, \bar{b}\bar{b} \rightarrow g, \\ \text{charge-aware:} & \quad bg \rightarrow b, \bar{b}g \rightarrow \bar{b}, b\bar{b} \rightarrow g, bb \rightarrow b, \bar{b}\bar{b} \rightarrow \bar{b}. \end{aligned} \quad (2)$$

Notice that in the charge-aware scheme the cross section does not receive contributions from initial state  $bb$  and  $\bar{b}\bar{b}$  processes, due to the requirement that there are at least 2  $b$  jets and 2 anti- $b$  jets in the final state. At the level of inclusive cross sections we find differences of the order of 1% with respect to simply ignoring initial state  $b$  contributions. However, at the differential level these could be sizable in certain

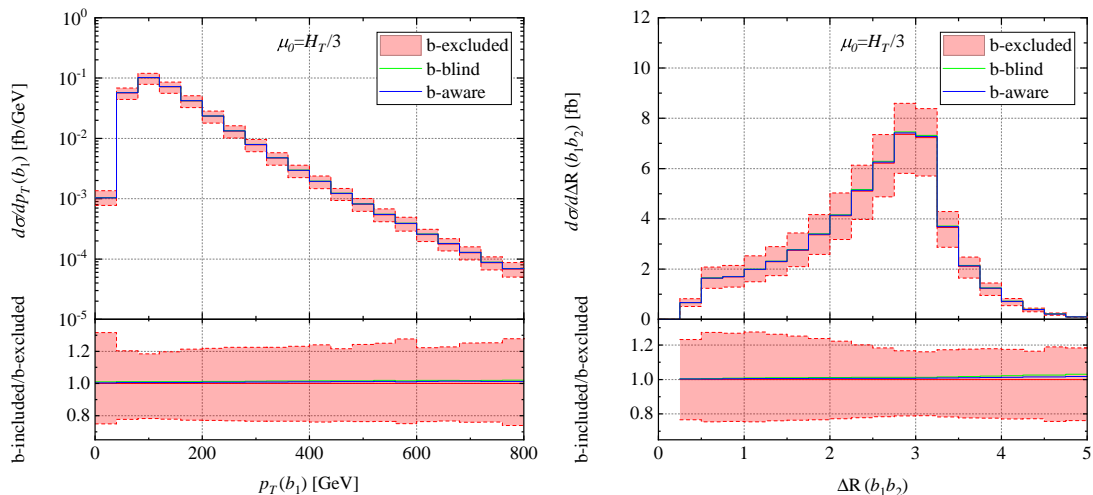


Figure 3: Differential cross section distribution for the transverse momentum of the hardest  $b$  jet (l.h.s) and the  $\Delta R$  separation of the two hardest  $b$  jets (r.h.s) for various  $b$  jet definitions. Plots taken from Ref. [13].

phase space regions. In Fig. 3 we show the impact of the various  $b$  jet definitions for the case of the transverse momentum of the hardest  $b$  jet as well as the  $\Delta R$  separation between the two hardest  $b$  jets. Also at the differential level we observe that initial state  $b$  contributions are negligible. Even in extreme phase space regions, for example  $\Delta R \gg 3$ , which could in principle be sensitive to the  $gb$  induced real radiation processes do not show a significant enhancement. Therefore, initial state  $b$  contributions are generally deemed negligible.

## 4 Conclusions

We highlighted some of the recent results [13] of our state-of-the-art calculation for off-shell  $pp \rightarrow t\bar{t}b\bar{b}$  production in the di-leptonic decay channel for the LHC at  $\sqrt{s} = 13$  TeV. We discussed briefly the outline of our calculation and the impact of NLO QCD corrections at the inclusive and differential level. We found large corrections of the order of +90% for the integrated cross section, while at the differential level they increase even further. The scale uncertainties are at the  $\pm 20\%$  level, while PDF uncertainties, which can amount up to a few percent are negligible in comparison. In addition, we also investigated the impact of different  $b$  jet definitions on our results. We found that our results are very stable with respect to modifications of the  $b$  jet definition and that initial state  $b$  contributions are overall negligible.

## References

- [1] A. Bredenstein, A. Denner, S. Dittmaier and S. Pozzorini, , *JHEP* **08** (2008) 108.
- [2] A. Bredenstein, A. Denner, S. Dittmaier and S. Pozzorini, , *Phys. Rev. Lett.* **103** (2009) 012002.
- [3] G. Bevilacqua, M. Czakon, C. G. Papadopoulos, R. Pittau and M. Worek, , *JHEP* **09** (2009) 109.
- [4] A. Bredenstein, A. Denner, S. Dittmaier and S. Pozzorini, , *JHEP* **03** (2010) 021.
- [5] M. Worek, , *JHEP* **02** (2012) 043.
- [6] A. Kardos and Z. Trócsányi, , *J. Phys. G* **41** (2014) 075005.
- [7] F. Cascioli, P. Maierhöfer, N. Moretti, S. Pozzorini and F. Siegert, , *Phys. Lett. B* **734** (2014) 210–214.
- [8] M. V. Garzelli, A. Kardos and Z. Trócsányi, , *JHEP* **03** (2015) 083.
- [9] G. Bevilacqua, M. V. Garzelli and A. Kardos, , 1709.06915.
- [10] T. Ježo, J. M. Lindert, N. Moretti and S. Pozzorini, , *Eur. Phys. J. C* **78** (2018) 502.
- [11] G. Bevilacqua and M. Worek, , *JHEP* **07** (2014) 135.
- [12] F. Buccioni, S. Kallweit, S. Pozzorini and M. F. Zoller, , *JHEP* **12** (2019) 015.

- [13] G. Bevilacqua, H.-Y. Bi, H. B. Hartanto, M. Kraus, M. Lupattelli and M. Worek, , [JHEP 08 \(2021\) 008](#).
- [14] A. Denner, J.-N. Lang and M. Pellen, , [Phys. Rev. D 104 \(2021\) 056018](#).
- [15] G. Bevilacqua, M. Czakon, M. V. Garzelli, A. van Hameren, A. Kardos, C. G. Papadopoulos et al., , [Comput. Phys. Commun. 184 \(2013\) 986–997](#).
- [16] G. Bevilacqua, H. B. Hartanto, M. Kraus and M. Worek, , [Phys. Rev. Lett. 116 \(2016\) 052003](#).
- [17] G. Bevilacqua, H. B. Hartanto, M. Kraus and M. Worek, , [JHEP 11 \(2016\) 098](#).
- [18] G. Bevilacqua, H. B. Hartanto, M. Kraus, T. Weber and M. Worek, , [JHEP 10 \(2018\) 158](#).
- [19] G. Bevilacqua, H. B. Hartanto, M. Kraus, T. Weber and M. Worek, , [JHEP 11 \(2019\) 001](#).
- [20] G. Bevilacqua, H.-Y. Bi, H. B. Hartanto, M. Kraus and M. Worek, , [JHEP 08 \(2020\) 043](#).
- [21] G. Ossola, C. G. Papadopoulos and R. Pittau, , [JHEP 03 \(2008\) 042](#).
- [22] A. van Hameren, C. G. Papadopoulos and R. Pittau, , [JHEP 09 \(2009\) 106](#).
- [23] A. van Hameren, , [Comput. Phys. Commun. 182 \(2011\) 2427–2438](#).
- [24] M. Czakon, C. G. Papadopoulos and M. Worek, , [JHEP 08 \(2009\) 085](#).
- [25] G. Bevilacqua, M. Czakon, M. Kubocz and M. Worek, , [JHEP 10 \(2013\) 204](#).
- [26] M. Czakon, H. B. Hartanto, M. Kraus and M. Worek, , [JHEP 06 \(2015\) 033](#).
- [27] M. Cacciari, G. P. Salam and G. Soyez, , [JHEP 04 \(2008\) 063](#).